Eur Biophys J (2001) 29: 559–568
DOI 10.1007/s002490000102

ARTICLE

**Stefano Della Longa · Alessandra Gambacurta
Alberto Bertollini · Marco Girasole
Agostina Congiu Castellano · Franca Ascoli**

Structure of the Fe-heme in the homodimeric hemoglobin from *Scapharca inaequivalvis* and in the T72I mutant: an X-ray absorption spectroscopic study at low temperature

Received: 8 February 2000 / Revised version: 9 August 2000 / Accepted: 9 August 2000 / Published online: 8 November 2000

Abstract The Fe site structure in the recombinant wild-type and T72I mutant of the cooperative homodimeric hemoglobin (HbI) of the mollusc *Scapharca inaequivalvis* has been investigated by measuring the Fe K-edge X-ray absorption near edge structure (XANES) spectra of their oxy, deoxy and carbonmonoxy derivatives, and the cryogenic photoproducts of the carbonmonoxy derivatives at $T = 12$ K. According to our results, the Fe site geometry in T72I HbI-CO is quite similar to that of human carbonmonoxy hemoglobin (HbA-CO), while in native HbI-CO it seems intermediate between that of HbA-CO and sperm whale MbCO. The XANES spectra of oxy and deoxy derivatives are similar to the homologous spectra of human HbA, except for T72I HbI, for which the absorption edge is blue-shifted (about +1 eV) towards the spectrum of the oxy form. XANES spectra of the cryogenic photoproducts of HbA-CO (HbA*), HbI-CO (HbI*) and mutant HbI-CO (T72I HbI*) were acquired under continuous illumination at 12 K. The Fe-heme structures of the three photoproducts are similar; however, while in the case of HbA* and HbI* the data indicate incomplete structural relaxation of the Fe-heme towards its deoxy-like (T) form, the relaxation in T72I HbI* is almost completely towards the proposed "high affinity" Fe-heme structure of T72I HbI. This evidence suggests that minor tertiary restraints affect the Fe-heme dynamics of T72I HbI, corresponding to a reduction of the energy necessary for the T → R structural transition, which can contribute to the observed dramatic enhancement in oxygen affinity of this hemoprotein, and the decreased cooperativity.

Key words Hemoproteins · Synchrotron radiation · Photolysis · X-ray absorption spectroscopy

S. Della Longa (✉)
Dipartimento di Medicina Sperimentale,
Università dell'Aquila, Via Vetoio, 67100 L'Aquila, Italy
E-mail: dlonga@fismedw2.univaq.it
Tel.: +39-0862-433568; Fax: +39-0862-433523

A. Gambacurta · F. Ascoli
Dipartimento di Medicina Sperimentale e Scienze Biochimiche,
Università di Roma "Tor Vergata",
Via di Tor Vergata 135, 00133 Rome, Italy

A. Bertollini
Dipartimento di Scienze Biochimiche,
Università di Roma "La Sapienza",
Piazzale A. Moro 5, 00185 Rome, Italy

M. Girasole
Istituto Struttura della Materia, CNR,
Via Fosso del Cavaliere, 00133 Rome, Italy

A. Congiu Castellano
Dipartimento di Fisica, Università di Roma "La Sapienza",
Piazzale A. Moro 5, 00185 Rome, Italy

S. Della Longa · M. Girasole · A. Congiu Castellano
INFM, Università di Roma "La Sapienza",
Piazzale A. Moro 5, 00185 Rome, Italy

Introduction

The homodimeric hemoglobin (HbI) from the bivalve mollusc *Scapharca inaequivalvis* has been the subject of numerous investigations because of the marked cooperativity in oxygen binding (Chiancone et al. 1981; Ikeda-Saito et al. 1983) that in vertebrates has been observed only in tetrameric hemoglobin. The X-ray structures of both the unliganded and liganded forms have been solved at high resolution (Royer et al. 1990; Royer 1994). The identical subunits closely resemble the myoglobin fold, whereas the quaternary structure is very different from that observed in vertebrate hemoglobins. The subunit interface is formed by the heme-carrying helices E and F, so that the two heme groups are in direct structural communication across this interface via a hydrogen-bond network, which involves a cluster of water molecules. The same study indicates that Phe97 (a residue in hydrogen-bond contact with the Nδ1 of the proximal histidine) is extruded towards the subunit interface upon ligand binding, and makes a close hydrophobic interaction with Thr72, suggesting that Phe97 plays a critical role in modulating oxygen affinity.

The T72I HbI mutant has been recently expressed with the aim to alter the subunit communication mechanism, by increasing the hydrophobic character of the interface. This mutant exhibits enhanced oxygen affinity, and markedly reduced cooperativity (Gambacurta et al. 1995); these functional changes have been accounted for by some subtle structural changes at the interface and by the key role of the interface water cluster, as revealed by X-ray structure studies at high resolution of the deoxy and CO mutant derivatives (Pardanani et al. 1998). As a matter of fact, the absence of the Thr72 hydroxyl group, which forms an H-bond with a water molecule in the subunit interface of the native deoxy protein, leads to the loss of two water molecules, and to a significant disordering of the inter-subunit water cluster, which strongly destabilizes the deoxy state of the mutant. On the other hand, spectroscopic studies (low-temperature visible absorption and resonance Raman) on the deoxy and CO forms and on the CO derivative photoproducts, as well as molecular dynamics studies, indicate a destabilization of the low affinity state in the mutant, with a heme more planar and a more rigid heme environment.

In this paper, we have attempted an X-ray absorption near edge structure (XANES) study of the recombinant wild-type and T72I mutant HbI, in order to elucidate the subtle structural differences at the Fe-heme site between the two proteins, with the aim to correlate them with the functional changes. X-ray absorption spectroscopy (XAS) probes photoelectron transitions from a deep metal core level to final unoccupied continuum states with selected symmetry formed by interference between the out-going photoelectron wave from the metal centre and the backscattering waves from neighbouring atoms. Hence it is very sensitive to the structure of the Fe-heme site (Pin et al. 1994). The XANES data presented here are interpreted by assuming that the Fe-heme geometry in the deoxy HbI mutant has been converted in a more relaxed, "high affinity", form. This fact can give a relevant contribution to the observed differences in oxygen binding parameters for the mutant.

Materials and methods

S. inaequivalvis HbI cDNA was expressed in JM105 *Escherichia coli* strain and the oxygenated holoprotein was purified as previously described (Gambacurta et al. 1993). The Ile mutant was obtained by site-directed mutagenesis on the HbI cDNA. Expression was performed in HB101 *E. coli* strain and the HbI mutant was purified as previously described (Gambacurta et al. 1995). The CO derivatives of the wild-type and mutant protein were obtained by equilibrating the oxy derivatives (in 0.1 M phosphate buffer, pH 7.0) under 1 atm of CO. Deoxy derivatives were obtained by addition of a few grains of dithionite to the oxygenated protein solutions, properly equilibrated under nitrogen gas. Visible absorption spectra (measured on a DMS 100 Varian spectrophotometer from 450 to 600 nm), registered on small amounts of the same samples used for the X-ray measurements, exhibited all the characteristic features of the oxy, deoxy and carbonmonoxy derivatives. Each XANES spectrum was collected by scans, and before averaging the scans it was verified that the last scan was identical to the first one. Protein concentration was about 5 mM in heme.

Fe K-edge XAS spectra were collected in fluorescence mode at the beam line D21 of the LURE synchrotron facility by using an energy-resolving array detector made by a seven-element Ge detector (Canberra Industries). The energy resolution at the Fe K_α fluorescence (6400 eV) was 170 eV. A Si(311) double crystal used as channel-cut was adopted as monochromator, and the spectral resolution at the Fe K-edge was about 1 eV. The spectra of the CO and deoxy derivatives (4 frames of about 601 experimental points with a $\Delta E = 0.2$ eV) have been acquired at 150 K and have a total signal averaging of 32 s/point. For the photolysis experiments the CO derivative samples were cooled at $T = 12$ K by using a liquid helium cryostat (model 22C Cryodine Cryocooler by CT Cryogenics, temperature controller model 80S by Lake Shore Cryotronics, and silicon diode temperature sensor DT-470-SD by Lake Shore). Photolysis was then achieved by prolonged illumination (white light) from a fibre optic illuminator for about 2 h. A UV/Vis microspectrophotometer was not available at the beam station, so we have only indirect indications that the samples were fully photolysed ($>95\%$). These are as follows:

1. At $T < 20$ K the steady state in photolysis kinetics corresponds to almost 100% of photolysis.
2. The calculated optical density of our sample changes from OD = 96 at 420 nm, to OD = 7 at 540 nm, and to OD = 0.05 at 630 nm, so that efficient photolysis on the sample is induced by photons between 500 and 600 nm.

The integrated power density of the fibre-optic illuminator between 500 and 600 nm was 5×10^{-2} mW mm^{-2}. The sample was maintained under illumination for the duration of the experiment [as in the protocol of Schlichting et al. (1994) on myoglobin crystals]. Before collecting the XAS spectra, distinct spectral changes at $E = 7124$ eV were monitored until a steady state was reached. The estimated photolysis rate for wavelengths between 500 and 600 nm was 0.002–0.2 s^{-1}. The kinetic curve of the X-ray absorption difference $[I_{7124}(t)–I_{7124}(0)]/[I_{7124}(\infty)–I_{7124}(0)]$ reached saturation in less than 1 h. The same saturation limit $I_{7124}(\infty)$ was obtained by changing the intensity of irradiation.

The fluorescence counts jumped from 70 counts s^{-1} element^{-1} before the edge (7100 eV), to about 850 counts s^{-1} element^{-1} above the edge (7250 eV), giving a total count jump of about 175,000 with a noise-to-signal ratio of 6×10^{-4} before the edge and 2×10^{-3} after the edge. In all experimental spectra the energy is aligned at the absorption threshold of metallic Fe foil. Alignment is checked contemporary to the acquisition of spectra by looking at two little glitches of the incident X-ray intensities located at 7136.6 ± 0.1 eV and 7148.0 ± 0.2 eV. The pre-edge was subtracted and the spectra were normalized at the extended X-ray absorption fine structure (EXAFS) limit of about 700–800 eV beyond the absorption threshold. This procedure leaves an uncertainty of some percent in the jump. After that, the spectra were all normalized again by minimizing the differences between all the spectra and that of the analogous derivative of sperm whale myoglobin or human hemoglobin, taken as reference. The normalization constant was used as a fitting parameter between each spectrum and the reference, by minimizing the differences. The goodness of this normalization procedure is shown in Fig. 1A, where the XANES spectra of the carbonmonoxy derivatives of horse myoglobin (hMbCO, solid curve) and sperm whale myoglobin (swMbCO, dotted curve) are superimposed. An enlargement in the range 7120–7180 eV is shown for the same spectra in Fig. 1B, for the spectra of swMbCO (dotted curve) and HbA-CO (solid curve) in Fig. 1C, and for the spectra of deoxy HbA (dotted curve) and HbI (solid curve) in Fig. 1D, as examples of the spectral differences studied.

We have measured the carbonmonoxy samples at $T = 150$ K to suppress both eventual X-ray damaging at higher temperature, and incidental undesired events of partial photolysis at lower temperature. As, in the present work, data on carbonmonoxy and deoxy

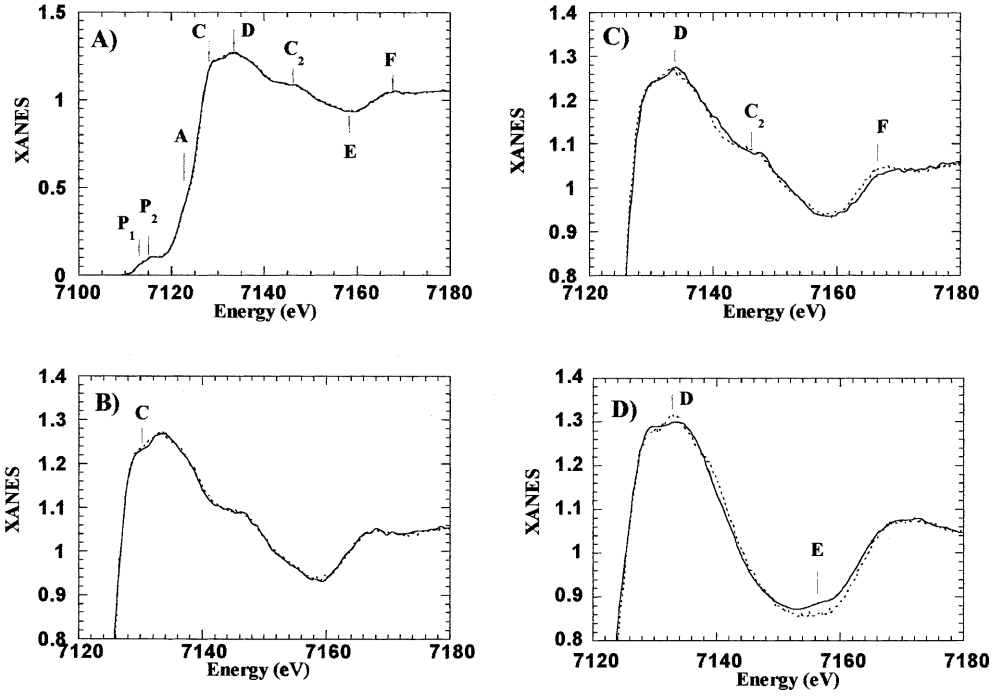

Fig. 1 **A** XANES spectra of swMbCO (*dotted curve*) and hMbCO (*solid curve*) and an enlargement of the XANES spectra of **B** swMbCO (*dotted curve*) and hMbCO (*solid curve*), **C** swMbCO (*dotted curve*) and HbA-CO (*solid curve*, *lower frame*) and **D** swMb (*dotted curve*) and HbI (*solid curve*)

derivative samples at $T = 150$ K have been compared with data on photoproducts at $T = 12$ K, a discussion on temperature effects seems necessary: although the effects of temperature on an XAS spectrum are well known in principle, no study has been reported on a protein system, as far as we are aware.

Nuclear vibrations induce exponential damping terms in the energy (or electron wavenumber, k) scale of an XAS spectrum. For a certain absorber-scatterer couple at a distance R_j, this damping factor in the single scattering theory of EXAFS is accounted for by the Debye-Waller term $[\exp(-2\sigma_j^2 k^2)]$; where σ_j is the root mean square (r.m.s.) deviation of R_j. It is related to the individual atomic displacements of the absorbing atom $\left(\left\langle |rm\vec{x}_{\mathrm{abs}}|^2 \right\rangle\right)$ and the scattering atom $\left(\left\langle |\vec{x}_{\mathrm{sca}}|^2 \right\rangle\right)$ by the following relationship:

$$\sigma_j^2 = \left\langle \left(\vec{x}_{\mathrm{abs}} \times \vec{r}_j\right)^2 \right\rangle + \left\langle \left(\vec{x}_{\mathrm{sca}} \times \vec{r}_j\right)^2 \right\rangle - 2\left\langle \left(\vec{x}_{\mathrm{obs}} \times \vec{r}_j\right)\left(\vec{x}_{\mathrm{sca}} \times \vec{r}_j\right) \right\rangle \quad (1)$$

where $\vec{r}_j$ is a unitary vector oriented like R_j. The last term of Eq. (1) includes correlated motions of the absorber-scatterer couple. The temperature dependence of the individual atomic displacements in Mb^+ is well known, including a thermal transition at $T \approx 200$ K giving evidence for the existence of substates (Hartmann et al. 1982). Nevertheless, the temperature dependence of σ_j is more limited, owing to the correlation term (D'Alba et al. 1990). The correlation tends to vanish for further shells, but in disordered systems like proteins only a few correlated shells contribute to the XAS signal. Temperature effects are relevant in the EXAFS energy range, while they are expected to be much less relevant in the short energy range of XANES. Other degrees of freedom in the multiple scattering regime of XANES, like rotation angles, neglected in Eq. (1), could contribute in principle to thermal damping. However, experimentally, temperature effects in the XANES range are found negligible in MbCO between 70 K and 300 K (unpublished observation), as well as in met-myoglobin between 30 K and 300 K (Della Longa et al. 1998). In this latter case, the thermal spin transition of alkaline met-myoglobin was probed spectroscopically as a perfect two-state transition, that would be impossible if relevant temperature effects would add to spin effects (like in UV-Vis spectra, strongly affected by vibronic coupling).

Results and discussion

Oxy derivatives

In Fig. 2A are shown the Fe K-edge XANES spectra of human HbA-O_2 (lower curve), native recombinant HbI-O_2 (centre curve) and T72I mutant HbI-O_2 (upper curve) in phosphate buffer at pH 7, $T = 150$ K. The energy position of the main features and of the absorption edge (defined by us as the energy where the XANES intensity measures 0.5 in normalized units) of the spectra are detailed in Table 1. The actual values for human hemoglobin can be different from the values reported in literature on the same derivatives [often referring to the first peak in the derivative spectrum (Pin et al. 1994, and references therein)] owing to our definition of the edge.

XANES spectra of the oxy derivatives are characterized by a single pre-peak P at 7113.4 eV. The spectra of Fig. 2A are largely similar; however, both the native and the mutant HbI-O_2 show a blue shift of the absorption edge of about 0.4 eV relative to HbA-O_2 (Table 1), as it appears from the negative broad peak at 7120–7125 eV of the difference spectra (Fig. 2B, Table 2). Edge shifts of hemoprotein XANES spectra are difficult to interpret without other independent information on the derivative under study. In fact they can occur depending on parameters changing contemporarily (Oyanagi et al. 1987; Della Longa et al. 1994), such as the iron coordination number, the average first neighbours distance, the Fe net charge and the Fe spin state. In the case of the oxy-hemoproteins compared in Fig. 2A, the spin state and the coordination numbers are

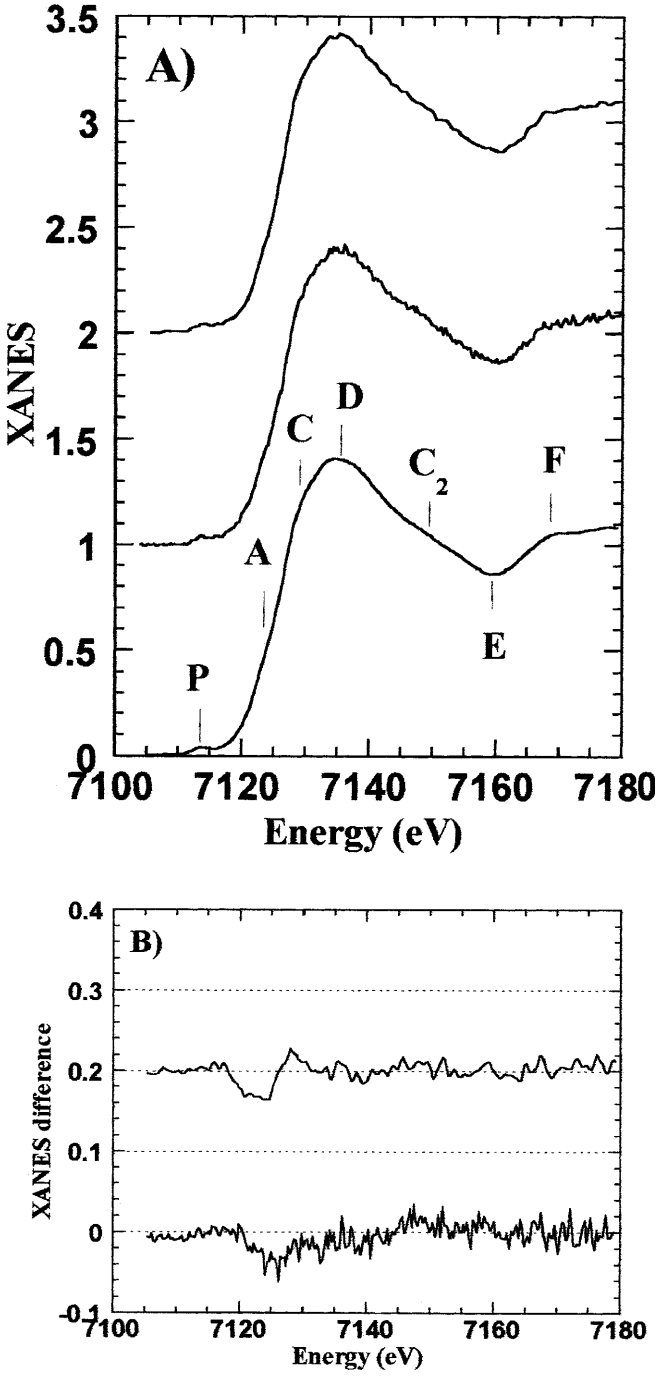

Fig. 2 **A** *From bottom to top*: XANES spectra of HbA-O_2, HbI-O_2 and T72I HbI-O_2. **B** XANES difference spectra of HbI-O_2–HbA-O_2 (*lower curve*) and T72I HbI-O_2–HbA-O_2 (*upper curve*)

the same; moreover, the Fe-N_p distance should be the same if the Fe lies always in-plane to a rigid undomed porphyrin ring. In such a case, the more reasonable explanation of the blue shift of the XANES edge of native and T72I HbI with respect to HbA-O_2 is a little increase of the Fe net charge, owing to back-donation occurring from the Fe to the oxygen molecule (Weiss 1964) and/or between Fe and the heme moiety, following ligand binding. An almost rigid shift of the XANES

Table 1 Energy positions (in eV) of the main peaks and edges of the XANES spectra of the oxy derivatives

Derivative	P	Edge[a]	C1[a]	D[a]	C2[b]	E[b]	F[b]
HbA(O_2)	7113.4	7123.8	7129.3	7135.0	7148	7159	7169
HbI(O_2)	7113.4	7124.2	7129.5	7135.0	7147	7160	7168
T72I HbI(O_2)	7113.4	7124.2	7129.2	7135.2	7148	7160	7168

[a] Energy error = 0.1 eV
[b] Energy error = 2 eV

Table 2 Intensity at a fixed energy of the XANES spectra of the oxy derivatives. Values expressed in normalized units (±0.005)

Derivative	7122 eV
HbA(O_2)	0.304
HbI(O_2)	0.282
T72I HbI(O_2)	0.275

spectrum without evident changes in shapes is observed in redox hemoproteins where the readjustment of the atomic environment that accompanies ligand-metal charge transfer is negligible, as in the case of oxidized and reduced cytochrome *c* (Cyt-*c*), for which the spectrum of reduced Cyt-*c* appears rigidly red-shifted relative to the one of oxidized Cyt-*c* (Labhardt and Yven 1979). Moreover, the red shift of the XANES edge of ferric *N*-methylimidazole cytochrome P-450-CAM, relative to that of *N*-methylimidazole myoglobin (the Fe-heme of the two proteins differing for the sixth iron ligand, cysteine thiolate in P-450, imidazole nitrogen in myoglobin), has been explained with the electron releasing character of the cysteine thiolate, i.e. by a transfer of electron density towards the Fe (Liu et al. 1995). According to our comparison of the oxy derivatives, a very small structural rearrangement at the iron site level seems to accompany the dramatic 40-fold increase of oxygen affinity measured for the oxy mutant with respect to the recombinant wild-type (Gambacurta et al. 1995).

Carbonmonoxy derivatives

In Fig. 3A, from bottom to top, the Fe K-edge XANES spectra of swMbCO, hMbCO, HbA-CO, native HbI-CO and T72I HbI-CO in phosphate buffer at pH 7.0, $T = 150$ K, are reported. Unlike the case of UV/V spectra, for which the transitions making the major contributions to the absorption intensity are almost completely polarized along the heme plane, making the spectra poorly dichroic, the polarized XANES spectra of swMbCO show a dramatic dichroism between a polarization of the X-ray photons nearly parallel and a polarization nearly perpendicular to the heme. Carbonmonoxy derivatives are characterized by the presence of two partially or totally resolved (depending on instrumental resolution) pre-edge peaks P_1 and P_2,

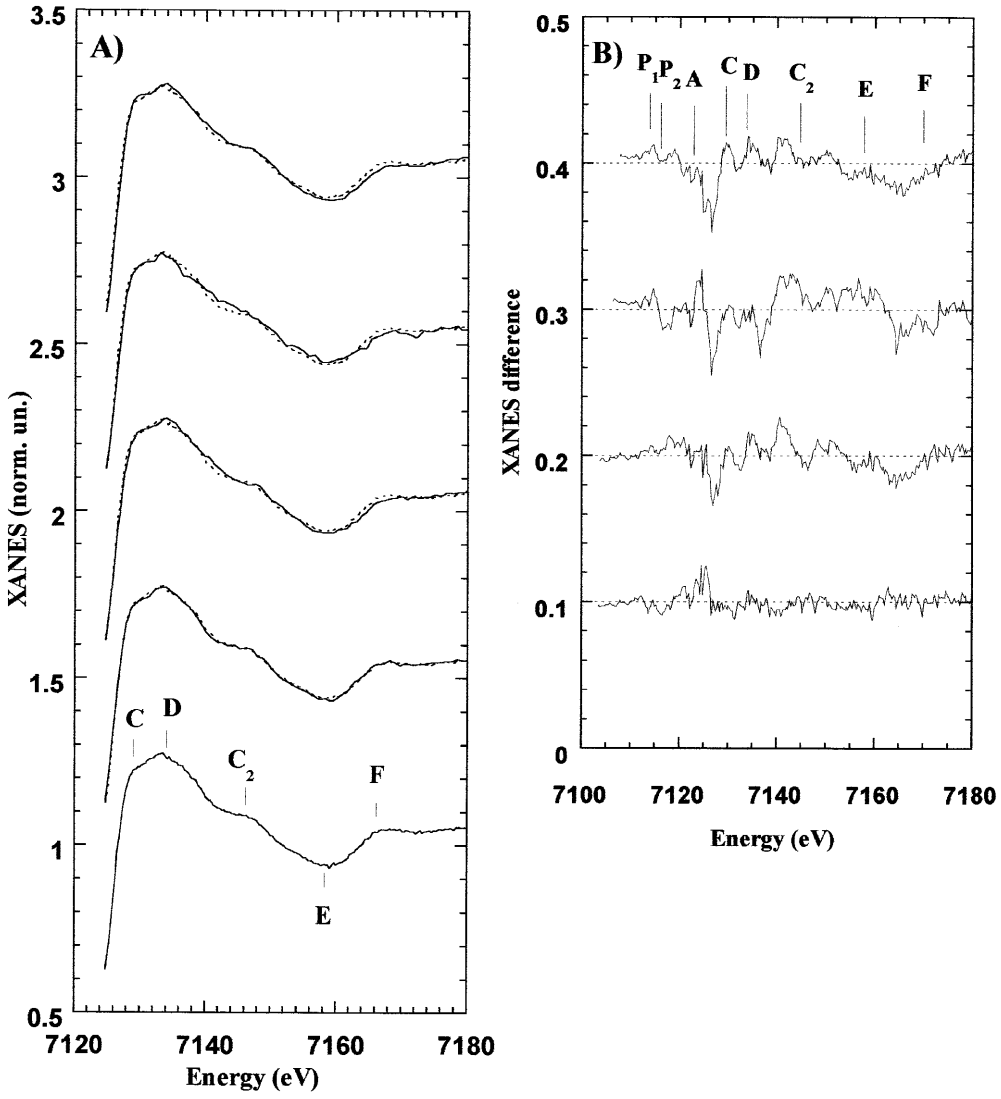

Fig. 3 **A** *From bottom to top*: XANES spectra of swMbCO, hMbCO, HbA-CO, HbI-CO and T72I HbI-CO. **B** *From bottom to top*: XANES difference spectra of hMbCO–swMbCO, HbA-CO–swMbCO, HbI-CO–swMbCO and T72I HbI-CO–swMbCO

the first polarized along the heme normal, and the second polarized on the heme plane. Peak P_1 has been assigned to a partially allowed (in an approximately C_{4v} symmetry) dipole transition from the core state 1s to the empty antibonding molecular orbital $CO(\sigma) + Fe(d_{z2})$. Peak P_2 has been assigned to a partially allowed dipole transition to the degenerate antibonding molecular orbital $CO(\pi^*) + Fe(d_{xz}, d_{yz})$ (Cartier et al. 1992). The strong peaks C_1 and C_2 are completely polarized along the heme normal so they probe the Fe-C-O and the Fe-His photoelectron pathways, being very sensitive to the Fe-C-O bond geometry; peak D is polarized on the heme plane and its intensity is expected to depend on heme doming effects in the dissociation process.

The energy positions of the various peaks are reported in Table 3. All the spectra are well aligned in

Table 3 Energy positions (in eV) of the main peaks and edges of the XANES spectra of the carbonmonoxy derivatives

Derivative	P1[a]	P2[a]	Edge[a]	C1[a]	D[a]	C2[b]	E[b]	F[b]
swMbCO	7113.0	7115.6	7123.8	7129.2	7133.2	7145	7158	7167
hMbCO	7113.0	7115.4	7123.6	7129.3	7133.2	7145	7158	7167
HbA-CO	7113.0	7115.5	7123.8	7129.5	7134.1	7147	7159	7169
HbI-CO	7113.0	7115.5	7123.8	7129.5	7133.8	7146	7160	7169
T72I HbI-CO	7113.1	7115.5	7123.9	7129.7	7133.8	7146	7159	7168

[a] Energy error = 0.1 eV
[b] Energy error = 2 eV

energy, the pre-peak P_1 lying always at 7113.0 ± 0.1 eV and the edge at 7123.8 ± 0.2 eV. The difference spectra between the latter four samples and swMbCO are reported in Fig. 3B. The XANES spectra of horse and sperm whale myoglobin are almost identical, with peaks at the same energy positions (Table 3) and the same intensities at fixed energies (Table 4), except for a small difference at 7123 eV. The difference pattern of HbA-CO exhibits more evident variations from swMbCO: the blue shift of peak D by about 1 eV (see also Fig. 1C), and the intensity changes at 7126, 7142 and 7166 eV, as reported in Table 4. Looking at the difference spectra of Fig. 3B, a complete similarity over all the XANES range emerges between the difference patterns relative to HbA-CO and T72I HbI-CO. The difference pattern of the native recombinant HbI-CO also resembles that of HbA-CO. In conclusion, the Fe site geometry in HbI-CO seems intermediate between that of swMbCO (or hMbCO) and that of HbA-CO, whereas in T72I HbI-CO is quite similar to that of HbA-CO.

The XANES differences between HbA-CO and swMbCO were previously interpreted as due simply to the difference in the Fe-CO bending angle (Bianconi et al. 1985), in accord with the X-ray diffraction determinations: α(Fe-CO) = 171–175° in the α and β subunits of HbA-CO (Derewenda et al. 1990) and α(Fe-CO) = 140° in swMbCO (Kuriyan et al. 1986). However, in the very recently reported X-ray structure of swMbCO at a resolution of 1.15 Å (Kachalova et al. 1999), the Fe-heme site, and the Fe-CO geometry in particular, with a bending angle α(Fe-CO) = 172°, is quite similar to the average of the α and β subunits in HbA-CO. This result agrees with other recent independent spectroscopic studies (Lim et al. 1995; Sage and Lee 1997). Hence it seems that the interpretation of the XANES difference between HbA-CO and swMbCO has to be changed. Notwithstanding peaks C and C_2 being theoretically very sensitive to the CO bending angle, other structural parameters (such as the Fe-C and Fe-His distances) can affect the shape and intensities of the same XANES features. Unfortunately, a theoretical multi-parameter simulation of the XANES spectra, that could solve these conformational changes, is still unsatisfactory. Even if a structural interpretation of the XANES spectra is more difficult than previously stated, it seems relevant the observation that two distinct Fe-heme states can be probed, the first type including swMbCO and hMbCO, and the second including HbA-CO, T72I HbI-CO and probably native HbI-CO. The similarity between the Fe-heme-CO structures of different hemoglobins with different quaternary structure is rather intriguing.

Table 4 Intensity at fixed energies (eV) of the XANES spectra of the carbonmonoxy derivatives. Values expressed in normalized units (± 0.005)

Derivative	7127	7130	7134	7142	7160	7166
swMbCO	1.038	1.234	1.265	1.128	0.943	1.040
hMbCO	1.040	1.230	1.269	1.119	0.939	1.040
HbA-CO	1.009	1.239	1.277	1.150	0.939	1.025
HbI-CO	1.005	1.235	1.265	1.151	0.947	1.020
T72I HbI-CO	1.007	1.245	1.280	1.143	0.932	1.021

Deoxy derivatives

In Fig. 4A are shown the Fe K-edge XANES spectra of the deoxy derivatives of swMb (curve 1), hMb (curve 2), HbA (curve 3), native HbI (curve 4) and T72I mutant HbI (curve 5) in the same solvent conditions. The K-XANES spectrum of swMb exhibits two pre-peaks P1 and P2 (typical of high-spin ferrous complexes) that are solvable by looking at the polarized spectrum of its crystal, and are located at 7112.5 and 7114.5 eV (data to be published). In our spectrum of the solution sample, only a single broader peak P at 7113.1 eV is discernible. The energy position of the main features of the spectra, P, C, D, D′, E and F, and of the edge, measured as well as for carbonmonoxy and oxy derivatives, are listed in Table 5. The intensities measured at fixed energy position are reported in Table 6. Compared to the spectra of the oxy- and carbonmonoxy mutants, the XANES differences between deoxy derivatives are bigger, suggesting that a larger number of parameter changes characterize the conformations of the various derivatives. The spectra of hMb is slightly but significantly different from swMb; peak C is 0.02 normalized units (n.u.) less intense, and the intensity at 7122 eV is 0.02 n.u. greater than swMb (Table 5). In HbA, peak A disappears; moreover, peak C is blue-shifted of 0.9 eV, and 0.01 n.u. more intense than swMb. The spectrum of native recombinant HbI exhibits larger differences: the absorption edge is 0.5 eV red-shifted, peak C has the same position than in HbA, but peak D is blue-shifted by 0.7–0.9 eV with respect to the first three globins, and the intensity at 7140 is 0.024–0.031 n.u. lower; the intensity increases significantly also between the features E and F.

Last, the XANES spectrum of T72I HbI shows important deviations from that of horse and sperm whale myoglobin. The absorption edge is blue-shifted by $+1$ eV with respect to myoglobins and human hemoglobin, and by $+1.4$ eV with respect to native HbI (Table 5). Owing to this fact, the spectral differences between T72I HbI and swMb are larger, showing a deep minimum at 7127 eV (Fig. 4B). It is well known that the edges of oxy and carbonmonoxy and ferric forms are blue-shifted, relative to those of the deoxy forms, by about 2.5, 3 and 4 eV, respectively (see also Table 7). The presence of fractions of met or oxy derivatives can be revealed, as the actual spectrum in this case can be obtained by a linear combination of the various derivatives, as in the case of oxy-HbA in the presence of the allosteric effectors inositol hexakisphosphate and bezafibrate together (Coletta et al. 1999). However, the blue shift of the spectrum of T74I HbI relative to the other deoxy derivatives cannot be explained by the presence of

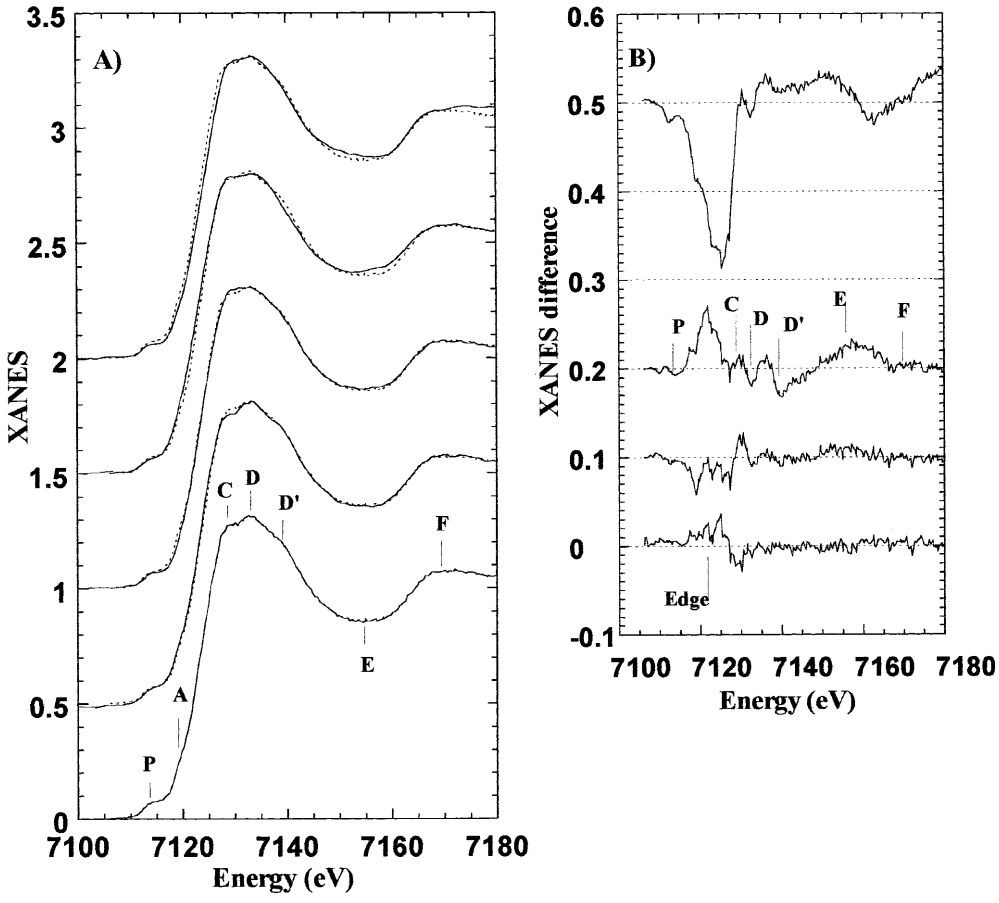

Fig. 4 **A** *From bottom to top*: XANES spectra of deoxy derivatives of swMb, hMb, HbA, HbI and T72I HbI. The spectrum of swMb is superimposed (*dotted line*) on the other spectra. **B** *From bottom to top*: XANES difference spectra of hMb–swMb, HbA–swMb, HbI–swMb and T72I HbI–swMb

Table 5 Energy positions (in eV) of the main peaks and edges of the XANES spectra of the deoxy derivatives

Derivative	P	Edge[a]	C1[a]	D[a]	D′[b]	E[b]	F[b]
swMb	7113.1	7121.3	7127.8	7132.1	7139	7153	7170
hMb	7113.1	7121.2	7127.8	7132.3	7139	7153	7170
HbA	7113.1	7121.3	7128.7	7132.3	7139	7154	7170
HbI	7113.1	7120.9	7128.8	7133.0	7139	7153	7170
T72I HbI	7113.3	7122.3	7130.3	7133.5	7139	7153	7170

[a] Energy error = 0.1 eV
[b] Energy error = 2 eV

Table 6 Intensity at fixed energies (eV). Values expressed in normalized units (±0.005)

Derivative	7113	7121.3	7129	7133	7140	7154	7170
swMb	0.055	0.505	1.274	1.313	1.165	0.858	1.074
hMb	0.053	0.526	1.254	1.308	1.165	0.858	1.077
HbA	0.050	0.506	1.288	1.308	1.158	0.863	1.075
HbI	0.052	0.572	1.283	1.299	1.134	0.874	1.075
T72I HbI	0.050	0.462	1.270	1.308	1.150	0.880	1.075

Table 7 Edge positions of the XANES spectra of the various derivatives (eV), and energy differences between the edges. Energy error = 0.1 eV

Derivative	Deoxy	CO	Oxy	CO–deoxy	Oxy–deoxy
swMb	7121.3	7123.8	–	+2.5	–
hMb	7121.2	7123.6	–	+2.4	–
HbA	7121.3	7123.8	7123.8	+2.5	+2.5
HbI	7120.9	7123.8	7124.2	+2.9	+3.3
T72I HbI	7122.3	7123.9	7124.2	+1.6	+1.9

fractions of met-HbI or oxy-HbI. As has been observed for oxy derivatives, in the case of unligated species with the same spin state, the effect can be explained either by partial charge transfer from/to the iron, or by a structural rearrangement, or both. Evidence of structural rearrangement, i.e. reduction of the Fe-heme displacement going from native to mutant HbI, has been reported by measuring the position of the "conformation sensitive" near-infrared band, positioned (at $T = 300$ K) at 760 nm in HbA and native HbI (Falconi et al. 1998), at 762 nm in swMb (Christian et al. 1997) and at 770 nm in T72I HbI. A correlation between the position of this band and the Fe-heme displacement reported by various crystallographic groups has been recognized (Christian et al. 1997, and references therein). On the other hand, the large similarity between low-frequency resonance Raman data of native and mutant HbI (Falconi et al. 1998) led to the suggestion that polarity effects (due to the presence of a water molecule or a hydroxyl ion in the

distal side) rather than structural rearrangements can be responsible for the blue shift of the IR conformational band (Christian et al. 1997). A deeper interpretation of the XANES spectra of the deoxy derivatives, and a connection to functional data, has been attempted by looking at the results of low-temperature carbon monoxide photolysis experiments described below.

Cryogenic photoproducts

In Fig. 5A are shown the Fe K-edge XANES spectra of human HbA-CO (dotted curve), HbA (dashed curve) and the cryogenic ($T = 12$ K) photoproducts HbA* (solid curve). The left inset shows an enhancement of the pre-peak region, while the right inset shows the difference spectra HbA*–HbA-CO (solid curve) and HbA–HbA-CO (dotted curve). Analogous spectra for native and mutant *Scapharca* hemoglobin are shown in Fig. 5B and C. The XANES spectra of the three cryogenic photoproducts, acquired under continuous illumination by a white light source at 12 K, are similar to each other, and similar to that measured for myoglobin (Della Longa et al. 1994). The photoproduct of carbonmonoxy myoglobin in these conditions is unligated, but the Fe-heme rearrangement towards the deoxy configuration is restrained at this temperature (Schlichting et al. 1994; Teng et al. 1997).

As previously stated during the discussion of the carbonmonoxy derivatives, the pre-edge features are assigned to dipole-forbidden 1s $\rightarrow$ d transitions to the first unoccupied states, i.e. the perturbed 3d states of the iron. These transitions have non-zero probability owing to various effects, the most effective being p-d mixing in a non-centrosymmetric coordination symmetry of the metal centre. For compounds with lower symmetry than approximate octahedral, p-d mixing increases and the pre-edge feature is expected to be enhanced. Five-coordinate compounds normally have a much higher intensity for the 1s $\rightarrow$ 3d transitions.

Because the HbCO $\rightarrow$ Hb reaction involves a low-spin $\rightarrow$ high-spin transition of the iron, one would expect peak P_1 to decrease in intensity because the electron occupation of the d_{z2} orbital changes from 0 to 1. At the same time, however, one expects the d-p mixing of the d_{z2} orbital to increase going from the pseudo-octahedral coordination symmetry in HbCO, to the square pyramidal coordination symmetry in Hb. This latter effect is opposite to the first and should limit the decreasing of peak P_1. As in the case of the d_{z2} orbital, the electron occupation of the d_{xy} orbital changes from 0 to 1 in the low-spin $\rightarrow$ high-spin transition, but the p-d mixing variations imposed by symmetry changes are certainly smaller than for the d_{z2} orbital. As a result, one expects a net decrease of peak P_2 due to the decrease of empty d states of *xy* symmetry.

The edge shift observed going from the CO derivatives to the photoproducts in Fig. 5A, B and C can be interpreted as follows: the red shifts of about 1.2–1.5 eV of the edge, consequent to ligand dissociation, probe the electronic relaxation of the quasi-bound states with p_z symmetry, as shown by the recent polarized XANES experiments on the low-temperature photoproduct of a swMbCO single crystal (Della Longa et al. 1999). The further Fe-heme relaxation towards the deoxy state should consist of atomic rearrangement to a conformation with higher Fe displacement and heme doming, parallel to a readjustment of the energy of the d electron states due to ligand field changes, determining the red shift of the pre-edge features in deoxy hemoglobin (left inset of Fig. 5A and B). However, while in the case of HbA* and HbI* the photoproduct represents a small percentage of the structural relaxation of the Fe-heme towards its deoxy-like (T) form, the relaxation of the T72I HbI* should be much more complete towards the proposed "high affinity" Fe-heme structure of T72I HbI (left inset of Fig. 5C).

As previously discussed, as the XANES shifts can be sensitive to polarity effects able to induce charge transfer from/to the iron centre, they cannot simply solve the discrepancy between resonance Raman and near-IR results (Falconi et al. 1998). We note here that, as reported by Christian et al. (1997), polarity effects only weakly affect the position of the conformation-sensitive band, so that structural effects on the near-IR probe seem dominant. Last, our XANES photolysis experiment has been made at low temperature in phosphate buffer in the absence of glycerol, so that solvent effects cannot be evoked in our case to destabilize the T-state in mutant HbI.

The conclusion of the present XANES study is in agreement with the suggestion that the T-like structure of the Fe-heme site in the mutant deoxy form has been destabilized towards a R-like, "high affinity" structure (Gambacurta et al. 1995). A Fe-heme average structure in T72I deoxy HbI more similar to that assumed in a ligated derivative could contribute to increase the oxygen affinity of the deoxy mutant. On the other hand, as explained above, according to the XANES comparison of the oxy derivatives, no structural rearrangement at the iron site level should be responsible for the increased affinity in the oxy mutant; hence polarity effects (i.e. a more hydrophobic heme environment, Falconi et al. 1998) seem a more convincing mechanism to explain the observed increase of oxygen affinity in T72I HbI with respect to the recombinant wild-type.

If minor tertiary restraints affect the Fe-heme dynamics of mutant HbI going from the deoxy to the oxy derivative, the decrease in cooperativity (as measured by the Hill coefficient, going from 1.5 in the native protein to 1.2 in the mutant) could be explained, at the Fe-heme site level, by a reduction of the proximal work that contributes to the T $\rightarrow$ R transition. As proposed by Champion and co-workers (Srajer et al. 1988; Champion 1989) in the Arrhenius expression for ligand binding rates of myoglobin, $k(\Delta H) = k_0 \exp(-\Delta H / k_B T)$, where k_B is the Boltzmann constant, the energy barrier ΔH can be expressed as the sum of two contributions:

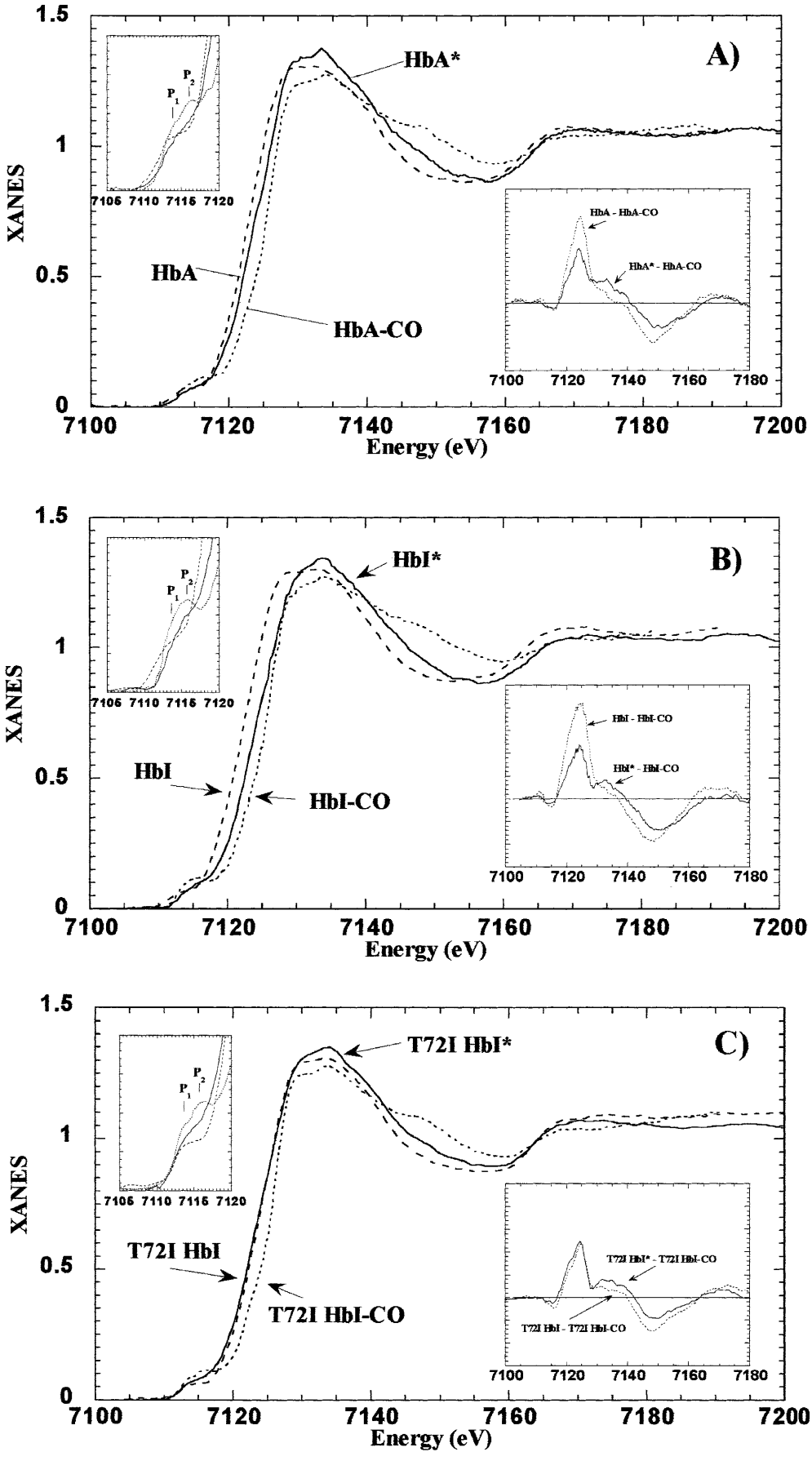

Fig. 5 **A** XANES spectra of HbA-CO (*dotted curve*), HbA* (*solid curve*) and HbA (*dashed curve*). In the *left inset* is an enlargement of the pre-edge features. In the *right inset* are the difference spectra of HbA*–HbA-CO (*solid curve*) and HbA–HbA-CO (*dotted curve*). **B** The same XANES spectra for native HbI. **C** The same XANES spectra for T72I HbI

$\Delta H = \Delta H_d + \Delta H_p$. The first term, ΔH_d, the distal work, includes energy barriers affecting ligand motions towards the iron site. The second term, ΔH_p, the proximal work, includes energy barriers affecting the readjustment of the Fe-heme-proximal histidine geometry. The proximal term can be roughly evaluated in an elastic approximation as $\Delta H_p = 0.5Ka^2$, in which a is the Fe-heme displacement and the constant K represents all the linear restoring forces involved in changing the Fe-heme structure toward a planar transition state. Thus, a reduction of the proximal term ΔH_p should contribute to decrease the change of the apparent binding affinity between the fully oxygenated and fully deoxygenated forms, i.e. the cooperativity.

Acknowledgements This work was supported by a grant from GNCB-CNR, Italy, by the EC's LIP programme and by MURST, Italy.

References

Bianconi A, Congiu-Castellano A, Durham PJ, Hasnain SS, Phillips S (1985) The CO bond angle in carboxymyoglobin determined by angular resolved XANES spectroscopy. Nature 318: 685–687

Cartier C, Momenteau M, Dartyge E, Fontaine A, Tourillon G, Bianconi A, Verdaguer M (1992) X-ray absorption spectroscopy of carbonyl basket handle Fe(II) porphyrins: the distortion of the tetrapyrrolic macrocycle. Biochim Biophys Acta 1119: 169–174

Champion PM (1989) Resonance Raman and site-directed mutagenesis studies of myoglobin dynamics. In: Jardetzky O (ed) Protein structure and engineering. (NATO ASI series, series A life sciences, vol. 183) Plenum Press, New York, pp 347–354

Chiancone E, Vecchini P, Verzili D, Ascoli F, Antonini E (1981) Dimeric and tetrameric hemoglobins from the mollusc *Scapharca inaequivalvis*. Structural and functional properties. J Mol Biol 152: 577–592

Christian JF, Unno M, Sage JT, Champion PM, Chien E, Sligar SG (1997) Spectroscopic effects of polarity and hydration in the distal heme pocket of deoxymyoglobin. Biochemistry 36: 11198–1120

Coletta M, Angeletti M, Ascenzi P, Bertollini A, Della Longa S, De Sanctis G, Priori AM, Santucci R, Amiconi G (1999) Coupling of the oxygen-linked interaction energy for inositol hexakisphosphate and bezafibrate binding to human HbA_0. J Biol Chem 274: 6865–6874

D'Alba G, Fornasini P, Rocca F, Mobilio S (1990) Temperature dependence of the EXAFS Debye-Waller factors of AgI. In: Balerna A, Bernieri E, Mobilio S (eds) 2nd European conference on progress in X-ray synchrotron radiation research. (Conference proceedings, vol 25) SIF, Bologna, pp 801–804

Della Longa S, Ascone I, Fontaine A, Congiu Castellano A, Bianconi A (1994) Intermediate states in ligand photodissociation of carboxymyoglobin by dispersive X-ray absorption. Eur Biophys J 23: 361–368

Della Longa S, Pin S, Cortes R, Soldatov AV, Alpert B (1998) Fe-heme conformations of ferric myoglobin. Biophys J 75: 3154–3162

Della Longa S, Arcovito A, Vallone B, Congiu Castellano A, Kahn R, Vicat J, Soldo Y, Hazemann JL (1999) Polarised X-ray absorption spectroscopy of the low temperature photoproduct of carbonmonoxy-myoglobin. J Synchrotron Radiat 6: 1138–1147

Derewenda Z, Dodson G, Emsley P, Harris D, Nagai K, Perutz M, Renaud JP (1990) Stereochemistry of carbon monoxide binding to normal human adult and Cowtown haemoglobins. J Mol Biol 211: 515–519

Falconi M, Desideri A, Cupane A, Leone M, Ciccotti G, Peterson ES, Friedman JM, Gambacurta A, Ascoli F (1998) Structural and dynamic properties of the homodimeric hemoglobin from *Scapharca inaequivalvis* Thr72 → Ile mutant: molecular dynamics simulation, low temperature visible absorption spectroscopy, and resonance Raman spectroscopy studies. Biophys J 75: 2489–2503

Gambacurta A, Piro MC, Ascoli F (1993) Cooperative homodimeric hemoglobin from *Scapharca inaequivalvis*. cDNA cloning and expression of the fully functional protein in *E. coli*. FEBS Lett 330: 90–94

Gambacurta A, Piro MC, Coletta M, Clementi ME, Polizio F, Desideri A, Santucci R, Ascoli F (1995) A single mutation (Thr72 → Ile) is crucial for the functional properties of the homodimeric co-operative haemoglobin from *Scapharca inaequivalvis*. J Mol Biol 248: 910–917

Hartmann H, Parak F, Steigemann W, Petsko GA, Ringe Ponzi D, Frauenfelder H (1982) Conformational substates in a protein: structure and dynamics of metmyoglobin at 80 K. Proc Natl Acad Sci USA 79: 4967–4971

Ikeda-Saito M, Yonetani T, Chiancone E, Ascoli F, Verzili D, Antonini E (1983) Thermodynamic properties of oxygen equilibria of dimeric and tetrameric hemoglobins from *Scapharca inaequivalvis*. J Mol Biol 15: 1009–1018

Kachalova GS, Popov AN, Bartunik HD (1999) A steric mechanism for inhibition of CO binding to heme proteins. Science 284: 473–476

Kuriyan J, Wilz S, Karplus M, Petsko GA (1986) X-ray structure and refinement of carbon-monoxy (Fe II)-myoglobin at 1.5 Å resolution. J Mol Biol 192: 133–154

Labhardt A, Yven C (1979) X-ray absorption edge fine structure spectroscopy of the active site haem of cytochrome *c*. Nature 277: 150–151

Lim M, Jackson TA, Anfinrud PA (1995) Binding of CO to myoglobin from a heme pocket docking site to form nearly linear Fe-C-O. Science 269: 962–966

Liu HI, Sono M, Kadkhodayan S, Hager LP, Hedman B, Hodgson KO, Dawson JH (1995) X-ray absorption near edge studies of cytochrome P-450-CAM, chloroperoxidase, and myoglobin. J Biol Chem 270: 10544–10550

Oyanagi H, Iizuka T, Matsushita T, Saigo S, Makino R, Ishimura Y, Ishiguro T (1987) Local structure of heme-iron studied by high-resolution XANES; thermal spin equilibrium in myoglobin. J Phys Soc Jpn 56: 3381–3388

Pardanani A, Gambacurta A, Ascoli F, Royer WE Jr (1998) Mutational destabilization of the critical interface water cluster in *Scapharca* dimeric hemolgobin: structural basis for altered llosteric activity. J Mol Biol 284: 729–739

Pin S, Alpert B, Congiu Castellano A, Della Longa S, Bianconi A (1994) XAS spectroscopy of hemoglobin. Methods Enzymol 232: 266–292

Royer WE Jr (1994) High resolution crystallographic analysis of a co-operative dimeric hemoglobin. J Mol Biol 235: 657–681

Royer WE Jr, Hendrickson WA, Chiancone E (1990) Structural transitions upon ligand binding in a cooperative dimeric hemoglobin. Science 249: 518–521

Sage JT, Jee W (1997) Structural characterization of the myoglobin active site using infrared crystallography. J Mol Biol 274: 21–26

Schlichting I, Berendzen J, Phillips GN Jr, Sweet RM (1994) Crystal structure of photolysed carbonmonoxy-myoglobin. Nature 371: 808–812

Srajer V, Reinisch L, Champion PM (1988) Protein fluctuations, distributed coupling and the binding of ligands to heme proteins. J Am Chem Soc 110: 6656–6670

Teng TY, Srajer V, Moffat K (1997) Initial trajectory of carbon monoxide after photodissociation from myoglobin at cryogenic temperatures. Biochemistry 36: 12087–12100

Weiss JJ (1964) Nature of the iron-oxygen bond in oxyhaemoglobin. Nature 202: 83–84